Journal of Chromatography, 217 (1981) 369–386
Elsevier Scientific Publishing Company, Amsterdam — Printed in The Netherlands

CHROM. 13,888

VERY-HIGH-SPEED LIQUID CHROMATOGRAPHY

II. SOME INSTRUMENTAL FACTORS INFLUENCING PERFORMANCE

JOSEPH L. DiCESARE*, MICHAEL W. DONG and JOHN G. ATWOOD
Chromatography Division, The Perkin-Elmer Corporation, Norwalk, CT 06856 (U.S.A.)

SUMMARY

Instrumental factors influencing very-high-speed liquid chromatography including injection volume, detector flowcell volume, detector response time and total instrumental bandwidth are discussed. Very-high-speed analyses performed using relatively short columns (100 mm) of conventional internal diameter (4.6 mm) packed with small particles (3 μm) result in very high performance as determined by the ability to generate over 400 theoretical plates/sec. Minimizing the total instrumental bandwidth by reducing volumes of the injector, connecting tubes and detector flowcell is necessary along with a very rapid detector response time in order to attain this performance. Limitations in performance on peaks having low capacity factors are apparent due to extra-column effects. The relatively high flow-rates which are utilized result in unexpectedly improved chromatographic performance since extra-column effects due to the flow path are not as great at higher flow-rates as originally expected. The largest contribution to extra-column effects appears to arise from the detector flowcell volume and the detector response time.

INTRODUCTION

Throughout the history of chromatography investigators have strived to increase liquid chromatographic (LC) performance by either increasing the efficiency of the separation, reducing the time required for the separation, or by a combination of both simultaneously. In a recent publication, we described an instrumental system for increasing chromatographic performance and discussed its capabilities[1]. The instrumental system utilized is similar to a conventional LC system in concept, except that the band-broadening or extra-column effects of the system have been reduced considerably. This is accomplished by reducing the volume of the sample flow path, *i.e.*, injection loop, connecting tubes and flowcell. In order to keep the system versatile and permit its use with most modes of LC, the first detector adapted for use with the system has been a variable-wavelength (190–600 nm) UV detector. The flowcell used in this detector has a total volume of 2.4 μl with optimized flow design and no dead volume. However, no compromise is made in sensitivity with this small-volume cell.

0021-9673/81/0000–0000/$02.50

as the signal-to-noise ratio of the detector is comparable to that of most conventional UV detectors having a much larger flowcell. Additionally, the double-beam optical design and holographic grating result in maximum stability and low stray light. In order to be compatible with very-high-speed chromatography, a very fast response time (135 msec) has also been incorporated into the electronics.

This high-speed instrumental system is utilized with small-dimensioned columns (*e.g.*, 100 × 4.6 mm I.D.) containing small-particle supports (3 or 5 μm) which permit very rapid analyses to be performed without sacrificing resolution relative to conventional systems. Other advantages of this system include enhanced sensitivity, reduced solvent consumption and rapid column re-equilibration times.

Very-high-speed analyses represent part of a trend toward the use of smaller volumes in LC. Another part of the trend is the development of very-small-bore columns of various types as described by Scott *et al.*[2–4], Tsuda and Novotny[5,6], Ishii and co-workers[7,8], Knox[9] and Tijssen[10]. In both of these types of LC, extra-column or band-broadening effects are extremely important; therefore, a thorough understanding of the causes of these effects is necessary.

In this paper, we examine some of the various instrumental parameters which impose limitations on very-high-speed LC mainly by virtue of their band-broadening or extra-column effects.

EXPERIMENTAL

A Perkin-Elmer Series 3B liquid chromatograph equipped with a Model LC-100 column oven and a Model LC-85 variable-wavelength UV/VIS detector (190–600 nm) was used. A 2.4-μl or a 8-μl flowcell was used interchangeably in the detector. A Perkin-Elmer Sigma 10 data station, Model 056 or Model 024 recorder or a Bascom-Turner (Newton, MA, U.S.A.) Model 8120 recorder capable of data acquisition rates of up to 1000 points/sec, were used for various experiments. Injections were accomplished using a Rheodyne Model 7125 injector equipped with either a standard 20-μl or a 6-μl sample loop made of 0.007 in. (0.18 mm) internal diameter tubing. Connecting tubing was all 0.007 in. (0.18 mm) internal diameter and a total of 80 cm length was used throughout the system. A 250 × 9 mm I.D. column filled with 55–105-μm high-surface-area silica was installed in the column oven between the pump and injector and served as a presaturation column[11]. For automated sample injections, a Perkin-Elmer Model 420 Auto Sampler having a Rheodyne 7413 injection valve with a 1.0-μl sample loop was used.

The columns used had an internal diameter of 4.6 mm and a length of 100 mm or 125 mm. The 100-mm columns were packed with 3-μm silica (Perkin-Elmer HS-3 silica, part number 0258-1500) or C_{18}-bonded phase (Perkin-Elmer HS-3 C_{18}, part number 0258-1501) supports. The 125-mm column was packed with 5-μm C_{18}-bonded phase (Perkin-Elmer HS-5 C_{18}, part number 0258-1001) support. The column characteristics have been described in more detail elsewhere[1].

HPLC-grade acetonitrile, chloroform and hexane from Fisher Scientific (Pittsburgh, PA, U.S.A.) was used for the mobile phases. Water was purified using a mixed-bed ion-exchange resin and an activated charcoal filter. Reference chemicals were of the highest purity available and were obtained from Aldrich (Milwaukee, WI,

U.S.A.), Eastman-Kodak (Rochester, NY, U.S.A.) and Pfaltz and Bauer (Stamford, CT, U.S.A.).

Instrumental bandwidth measurements were performed by injecting a solute (uracil or benzene) into the LC system where the column is replaced by a zero-dead-volume connecting union. Measurements of instrumental bandwidth (4σ peak volume) were obtained by measuring peak widths at half-height and multiplying by a factor of 1.7.

RESULTS AND DISCUSSION

An example of a very-high-speed liquid column chromatographic separation using a C_{18}-bonded phase support containing 3-μm particles is shown in Fig. 1, where a test mixture containing seven major components is separated in about 80 seconds. The final eluting component has a capacity factor (k) of 6.6 and the efficiency achieved is greater than 13,600 plates on the final peak. The column used was 100 × 4.6 mm I.D. and the volumetric flow-rate of the acetonitrile–water (65:35) mobile phase was 4.4 ml/min (linear velocity, u = 9.7 mm/sec). The operating inlet backpressure was 5000 p.s.i.g. (35 MPa) at 40°C. An example of a similar very-high-speed separation using a sillica support containing 3-μm particles is shown in Fig. 2, where a test mixture containing four components is separated in less than 60 sec. The final eluting component has a k value of 3.3 and the efficiency is over 9000 plates on the last peak. This column used was also 100 × 4.6 mm I.D. and the volumetric flow-

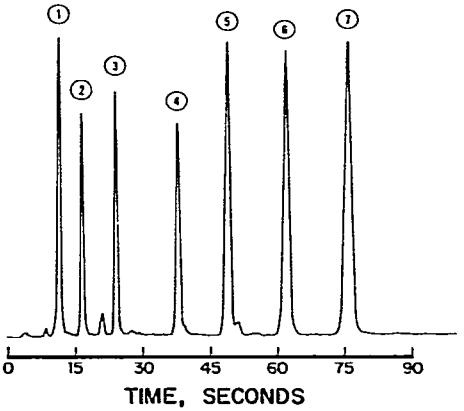

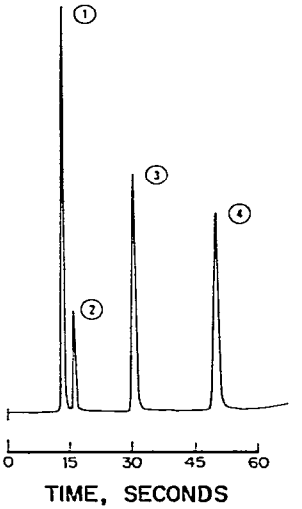

Fig. 1. Analysis of a test mixture, on a reversed-phase column. Column: 100 × 4.6 mm I.D., C_{18}-bonded phase packing, 3-μm particles. Mobile phase: acetonitrile–water (65:35) at 4.4 ml/min; inlet pressure: 5000 p.s.i.g. (35 MPa). Column temperature: 40°C. UV detector at 254 nm. Peaks: 1 = uracil (2,4-dioxopyrimidine); 2 = phenol; 3 = nitrobenzene; 4 = toluene; 5 = ethylbenzene; 6 = isopropylbenzene; 7 = *tert.*-butylbenzene.

Fig. 2. Analysis of a test mixture on a normal-phase column. Column: 100 × 4.6 mm I.D., silica packing, 3-μm particles. Mobile phase: chloroform–hexane (6:94) at 5.0 ml/min, inlet pressure: 2800 p.s.i.g. (20 MPa). Ambient temperature. UV detector at 254 nm. Peaks: 1 = benzene; 2 = biphenyl; 3 = azobenzene; 4 = nitrobenzene.

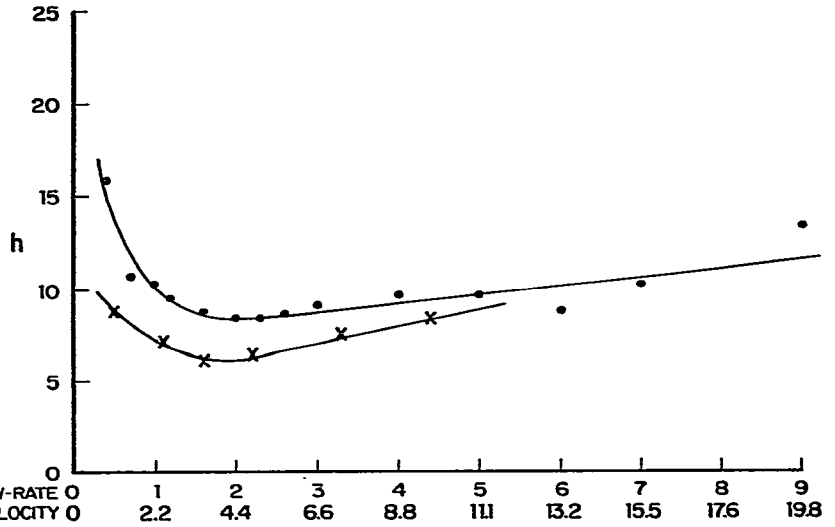

Fig. 3. Relationship of the plate height to the mobile phase linear velocity (flow-rate). Columns: 100 × 4.6 mm I.D., C_{18}-bonded phase (×) and silica (●) packing; 3-μm particles. Mobile phase: acetonitrile–water (65:35) (40°C) for C_{18} and chloroform–hexane (6:94) (ambient temperature) for silica. Solutes: × = *tert.*-butylbenzene (k = 6.6); ● = nitrobenzene (k = 3.3). Plate height is given in μm, linear velocity in mm/sec, and flow-rate in ml/min.

rate of the chloroform–hexane (6:94) mobile phase was 5.0 ml/min (u = 11.1 mm/sec). The operating inlet backpressure was 2800 p.s.i.g. (20 MPa) at ambient temperature.

These efficiencies in such short time periods could not be achieved on conventional LC systems. The attainment of this type of high chromatographic performance is due to:

(a) small particle supports (*e.g.* 3 μm) which generate the high efficiencies at high velocities of mobile phase in relatively short column lengths,

(b) small-diameter columns and their low void volumes which result in low mobile phase consumption and high mass sensitivity, and

(c) an instrumental system having minimized band-broadening effects which permits the high column efficiencies to be maintained.

The small-particle supports utilized are evaluated in Fig. 3 where plate height (h) is plotted *versus* mobile phase volumetric flow-rate and linear velocity. The minimum plate heights attained were 6.1 μm and 8.4 μm for the C_{18}-bonded phase and silica packings, respectively. This is equivalent to reduced plate heights of about 2 d_p and 2.8 d_p, respectively (where d_p is the average particle diameter) which indicates that the columns are packed very well. Additionally, the flow-resistance values for these columns are approximately 600 and 430 for the C_{18}-bonded phase and silica, respectively, thereby permitting operation at relatively high mobile phase linear velocities while not generating excessive inlet backpressures. As indicated in Fig. 3, the optimum linear velocities are relatively high, between 4 and 5 mm/sec (1.8 to 2.3 ml/min) as expected with small particles and the mass transfer term (C term of the Van Deemter equation) is quite low, making these packings ideally suited for very-high-speed liquid chromatography.

Chromatographic performance is probably best defined as suggested by Desty *et al.*[12] as the rate of production of theoretical plates (n) or effective plates (N), i.e., the ratio of theoretical plate number to the retention time (t_R)

$$\upsilon = n/t_R \tag{1}$$

or the ratio of the effective plate number to the retention time,

$$Y = N/t_R \tag{2}$$

where υ and Y represent the rate of production of the respective plate numbers. As previously discussed[1], the υ and Y terms are related to the three basic parameters of a peak: its retention time, its variance and its capacity factor.

The chromatographic performance demonstrated in Figs. 1 and 2 can, therefore, be best described by the rate of production of theoretical plates (n) or effective plates (N). These calculations are shown in Tables I and II and the results are plotted in Figs. 4–7. Table I shows the results for the C_{18} bonded phase column at flow-rates of 3.3 and 4.4 ml/min (u = 7.3 and 9.7 mm/sec) at 40°C. The best results are obtained at the higher flow-rate and are plotted as the rate of production of theoretical plates (Fig. 4) and effective plates (Fig. 5) *versus* k. The highest values reported, 352 theoretical plates/sec, and 167 effective plates/sec for the bonded phase, and 444 and 150, respectively, for the silica are believed to surpass any previously reported experimental data in the literature except for some work of Desty[12] using short (1–8.5 m) glass capillary open tubular gas chromatographic columns having a small internal diameter and a very thin stationary phase.

TABLE I

ANALYSIS OF REVERSED-PHASE CHROMATOGRAM

Conditions: A: flow-rate, 3.3 ml/min (u = 7.3 mm/sec); t_0 = 13.6 sec; ΔP = 3700 p.s.i.g. (26 MPa). B: flow-rate, 4.4 ml/min (u = 9.7 mm/sec); t_0 = 10.2 sec; ΔP = 5000 p.s.i.g. (35 MPa). Symbols: t_R = retention time, k = capacity factor, n = number of theoretical plates, $\upsilon = n/t_R$, N = number of effective plates, $Y = N/t_R$.

Conditions	*Peak*	t_R *(sec)*	k	n	υ	N	Y
A	1	16.2	0.24	3338	206	125	8
	2	22.2	0.71	5735	258	989	46
	3	32.4	1.47	9559	295	3386	105
	4	50.4	2.82	12,764	253	6956	138
	5	64.8	3.94	13,351	206	8493	131
	6	81.6	5.24	14,056	172	9912	122
	7	99.0	6.59	14,729	149	11,104	112
B	1	12.6	0.24	3016	239	113	9
	2	17.4	0.71	5162	297	890	51
	3	25.2	1.47	8864	352	3140	125
	4	39.0	2.82	11,943	306	6509	167
	5	50.4	3.94	12,065	239	7675	153
	6	63.6	5.24	12,861	203	9069	143
	7	77.4	6.59	13,637	176	10,280	133

TABLE II

ANALYSIS OF NORMAL-PHASE CHROMATOGRAM

Conditions: A: flow-rate, 3.0 ml/min (u = 6.6 mm/sec); t_0 = 15 sec; ΔP = 1700 p.s.i.g. (12 MPa). B: flow-rate, 5.0 ml/min (u = 11.1 mm/sec); t_0 = 9 sec; ΔP = 2800 p.s.i.g. (20 MPa). C: flow-rate, 7.0 ml/min (u = 15.5 mm/sec); t_0 = 7.0 sec; ΔP = 4100 p.s.i.g. (28 MPa). Symbols as in Table I.

Conditions	*Peak*	t_R *(sec)*	k	n	υ	N	Y
A	1	28.2	0.8	8163	286	1616	57
	2	31.8	1.1	8350	263	2288	72
	3	47.4	1.9	9832	260	4218	89
	4	71.4	3.3	10,959	153	6455	90
B	1	22.8	0.8	7584	314	1501	66
	2	25.2	1.1	7721	291	2116	84
	3	37.2	1.9	8612	251	3695	99
	4	55.2	3.3	10,370	187	6108	111
C	1	13.2	0.8	5589	431	1107	84
	2	15.0	1.1	6572	444	1801	120
	3	24.6	1.9	8586	348	3683	150
	4	37.2	3.3	9722	261	5726	154

Table II shows the results for the silica packing at flow-rates of 3, 5 and 7 ml/min (u = 6.6, 11.1, and 15.5 mm/sec). Again, better results are obtained as the flow-rate increases, indicative of the relatively low stationary phase mass transfer term. This indicates that the loss in plates as a function of increased flow-rate is not as great as the decrease in analysis time brought about by higher flow-rates.

Also plotted in Figs. 4–7 are the theoretically predicted data in terms of υ and Y for these columns plotted as a function of k. The theoretical data are derived as follows. First, assume that the column efficiency is independent of k for these small-particle supports[13]. From the actual theoretical plate numbers obtained (Tables I and

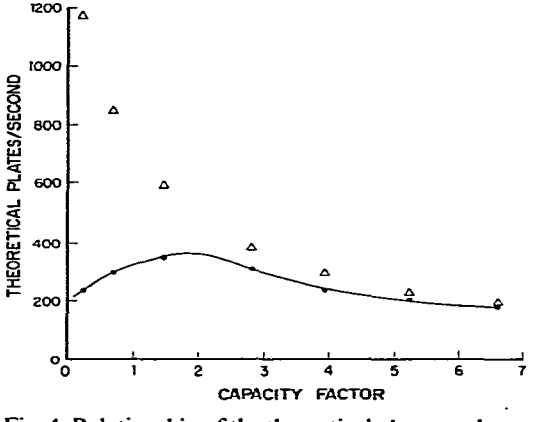

Fig. 4. Relationship of the theoretical plate number per second to the capacity factor for C_{18}-bonded phase packing. Column dimensions and conditions as in Fig. 1. △, Theoretical data; ●, experimental data.

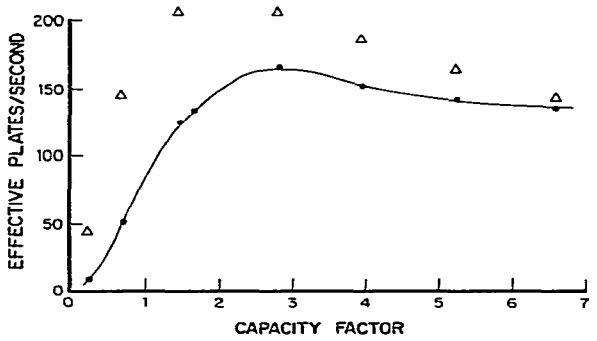

Fig. 5. Relationship of the effective plate number per second to the capacity factor for C_{18}-bonded phase packing. Column dimensions and conditions as in Fig. 1. △, Theoretical data; ●, experimental data.

II) the true column theoretical plate count is estimated from the following simultaneous equations:

$$n_i = \frac{5.54\,(1 + k_i)^2\,V_0^2}{(1 + k_i)^2\,w_0^2 + w_I^2} \tag{3}$$

$$n' = 5.54\,V_0^2/w_0^2 \tag{4}$$

(where w_0 and w_I are the bandwidths at half-height for the unretained peak for the column and the instrumental bandwidth respectively, n_i and k_i are measured plates and k for the ith peak, and V_0 is the column void volume). This indicates that the true number of theoretical plates n' per column (independent of extra-column effects) should be 14,900 and 11,700 for the C_{18}-bonded phase and silica, respectively, at 4.4

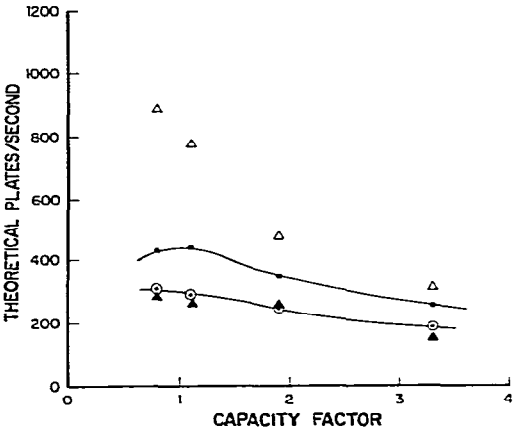

Fig. 6. Relationship of the theoretical plate number per second to the capacity factor for the silica packing. Column dimensions and conditions as in Fig. 2. △, Theoretical data; ●, data obtained at 7 ml/min (u = 15.5 mm/sec); ⊙, data obtained at 5 ml/min (u = 11.1 mm/sec); ▲, data obtained at 3 ml/min (u = 6.6 mm/sec).

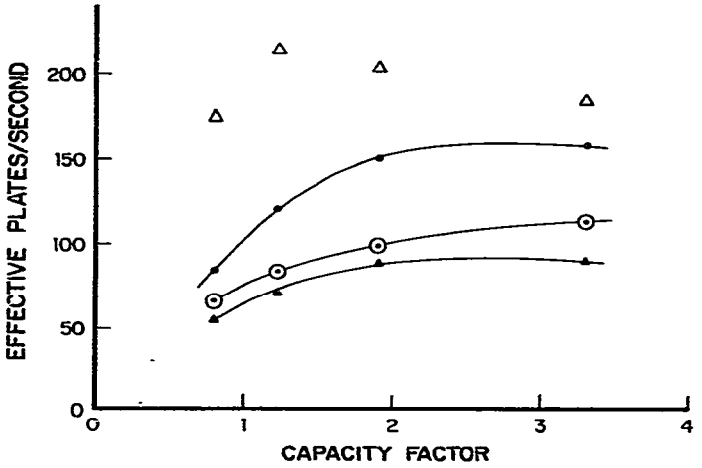

Fig. 7. Relationship of the effective plate number per second to the capacity factor for the silica packing. Column dimensions and conditions as in Fig. 2. Symbols as in Fig. 6.

ml/min and 7.0 ml/min. Then, assuming that the column efficiency is constant, independent of k, the theoretical values for the production of theoretical plates and effective plates are

$$v' = n'/t_R \tag{5}$$

$$Y' = N'/t_R \tag{6}$$

These values should follow the functions:

$$v' \approx \frac{1}{1 + k} \tag{7}$$

$$Y' \approx \frac{k^2}{(1 + k)^3} \tag{8}$$

As indicated in Figs. 4–7 the experimental data approaches the theoretical data as k increases while the difference between the experimental and theoretical data becomes greater and greater as k decreases. The cause of this is extra-column or band-broadening effects of the instrumental system which are essentially independent of k but have a greater influence as k decreases due to the smaller volume of the eluting peaks as shown in eqn. 9 where w_{95} is the bandwidth containing 95% of the peak area:

$$w_{95} = \frac{4\,(1 + k)\,V_0}{\sqrt{n}} \tag{9}$$

Performance can be expected to increase as particle size decreases even further. However the limitations in chromatographic performance appear to be two-fold at

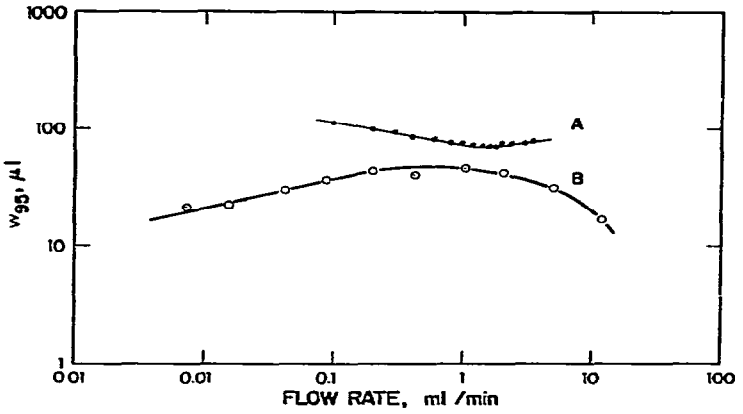

Fig. 8. Relationship of the instrumental bandwidth (w_{95}) and column bandwidth to the mobile phase flow-rate. Column as in Fig. 1; w_{95} as defined in the text. A, 3-µm C_{18}-bonded phase column at k = 1.8; B, instrumental bandwidth. Mobile phase: isopropanol. Solute: sodium benzoate, 0.5 mg/ml.

this time. Pressure limitations of pumping systems will determine the maximum flow-rates attainable. This is already becoming a limitation using more viscous solvents at high flow-rates with the C_{18}-bonded phase column. At a flow-rate of 5.0 ml/min at 40°C using acetonitrile–water (65:35), pressure approaching 6000 p.s.i.g. (42 MPa) is required. Of more consequence at this time is the loss in theoretical plates at low k values due to extra-column effects. These effects include band-broadening caused by the injection system, connecting tubes, detector flowcell, and response times of the detector and recorder/data handling device.

Instrumental bandwidth

The instrumental bandwidth (*IBW* or w_{95}) or extra-column effects of the system is determined by injecting solute into the chromatograph with the column

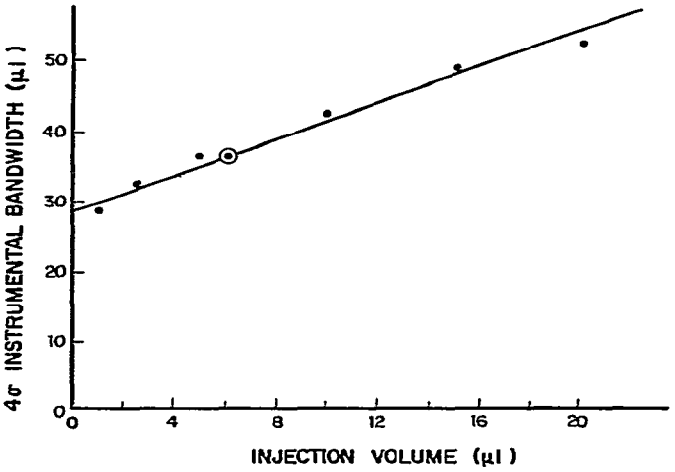

Fig. 9. Relationship of the instrumental bandwidth (w_{95}) to the injected sample volume. ●, Injections using 20-µl sample loop partially filled; ⊙, injection completely filling 6-µl loop.

removed from the system and measuring the volume in which it elutes at the detector. Methods for measuring and expressing the instrumental bandwidth previously have been discussed[4,14,15]. Considerable discrepancies can exist between the various methods of measurement and the most accurate results are obtained using the second moment analysis. However, since peak shapes were quite consistent, for comparative purposes we have used the peak width at half-height method for the measurements reported below. In Fig. 8 the w_{95} bandwidth of the C_{18}-bonded phase column at a k of 1.8 is plotted along with the instrumental bandwidth *versus* volumetric flow-rate. The column bandwidths are determined from eqns. 3, 4 and 9 and follow the shape of the Van Deemter plots for these columns. The *IBW*, however, does not increase linearly as expected with flow-rate[16], but, instead tends to decrease at higher flow-rates[17]. The shape of this curve varies somewhat with solvent viscosity but the general characteristics remain the same[18]. The fact that the *IBW* does not increase significantly as expected[16] at higher flow-rates permits highly efficient very-high-speed LC to be possible at this time using more or less conventional hardware.

Injection volume

The contribution of the sample injection to band broadening has previously been discussed by many workers[14,19–21]. Some compromise must be made between concentration detection limits which decreases as more sample mass is injected up to the column's capacity, and resolution which decreases as the sample volume increases due to an increase in instrumental bandwidth[22]. For a plug-type injection, which is believed to cause minimal band broadening[19], the variance expressed in volume units is:

$$\sigma_{inj}^2 = V_{inj}^2/12 \tag{10}$$

where V_{inj} is the injected volume and σ_{inj}^2 the variance of the injection. It has been shown that V_{inj} is directly proportional to the standard deviation, σ_{inj}, of the injection profile:

$$V_{inj} = K\,\sigma_{inj} \tag{11}$$

where K is a characteristic of the method of injection[21]. For a true plug injection K is equal to 3.5; however, experimental values obtained have generally been lower[20,22]. An analysis of the data in Fig. 9, where instrumental bandwidth is plotted *versus* injection volume results in a value for K of between 1 and 2. This is obtained by extrapolating to zero injection volume to determine the band broadening due to components other than the injector and then determining the contribution of the injector to the total band broadening at various injection volumes. As indicated in the figure the contribution from the injector appears to increase approximately linearly with increasing injection volume. The inability to obtain a true plug injection is believed to be due to the parabolic velocity profile in the injector. Techniques which tend to disrupt the parabolic velocity profile, such as coiling the sample loop to increase secondary flow[10,23], using a loop packed with glass beads[21] or using a temporary injection[21,24–26] will cause the variance of the injector to decrease and for the value of K to approach the theoretical value. These techniques apply to very-high-

TABLE III

INFLUENCE OF INJECTION VOLUME ON INSTRUMENTAL BANDWIDTH

Injection volume (μl)	*Instrumental bandwidth (μl)**	
	Flow-rate (ml/min)	
	1.0	*5.0*
3.0	30	–
6.0	31	38
10.0	36	–
13.5	37	42
23.5	47	48
50	86	85
100	160	147

* w_{95} or volume containing 95% of peak area.

speed LC as well. As the linear velocity of the mobile phase increases to very high levels, secondary flow can be expected to result in a lower variance from the injection process. A comparison of the contribution of injection volume to the total instrumental bandwidth (Table III) at flow-rates of 1.0 and 5.0 ml/min indicates that this does occur.

Connecting tubes and unions

The effect of connecting tubes has been studied by Martin *et al.*[27] and by Scott and Kucera[28]. As noted, short columns are more demanding than larger conventional columns and the connecting tube volumes should be kept as low as possible.

TABLE IV

CONTRIBUTION OF CONNECTING TUBING AND UNIONS TO INSTRUMENTAL BANDWIDTH

Basic system: 6-μl injection loop; 80 cm of 0.007-in. I.D. tubing; LC-85 UV detector with 2.4-μl flowcell.

System	*Instrumental bandwith (μl)**	
	Flow-rate (ml/min)	
	1.0	*5.0*
Basic	31	37
Basic plus 40 mm tubing plus 1 union	31	37
Basic plus 80 mm tubing plus 2 unions	32	38
Basic plus 300 mm tubing plus 1 union	37	39
Basic plus 500 mm tubing plus 2 unions	41	39
Basic plus 1 m tubing plus 1 union	44	49

* w_{95} or volume containing 95% of peak area.

The contribution of connecting tubing to band broadening can be determined from the Golay equation:

$$h = \frac{2 D_M}{u} + \frac{r^2 u}{24 D_M} \tag{12}$$

as shown by Martin *et al.*[27]

$$\sigma^2 = (\pi r^2)^2 L h \tag{13}$$

where D_M is the solute diffusivity, r the tube radius, h the height equivalent to a theoretical plate, and L the tube length. However, the prediction that the variance increases proportionally to increasing flow-rate[27] was found not to hold true for very high volumetric flow-rates due to secondary flow in short tube lengths[17]. Table IV shows the contribution of various lengths of 0.007-in. tubing and zero-dead-volume unions to the total instrumental bandwidth of the basic system (injector, 80 cm of 0.007-in. tubing, and detector). The contribution of the tubing to the total bandwidth increases with increasing tubing length; however, the increase is approximately the same for flow-rates of 1 and 5 ml/min. The contribution of the zero-dead-volume unions to the total bandwidth is insignificant.

Detector flowcell

The largest contribution to extra-column band-broadening results from the detector flowcell. The volume and the flow characteristics of the cell are both important. Ideally, the cell volume should be small and no dead volume should exist. We have examined the effect of two different flowcells on the total instrumental bandwidth. The results are shown in Fig. 10. The smaller cell, which is used in the Model LC-85 for high-speed chromatography, has a total volume of 2.4 μl. For comparison, a larger cell, typical of that used in a conventional UV detector was also used. The larger cell had an illuminated volume of 8 μl and a total volume slightly greater. As shown in Fig. 10, the reduction in instrumental bandwidth resulting from the smaller flowcell was quite dramatic. The instrumental bandwidth, w_{95}, was reduced from 72

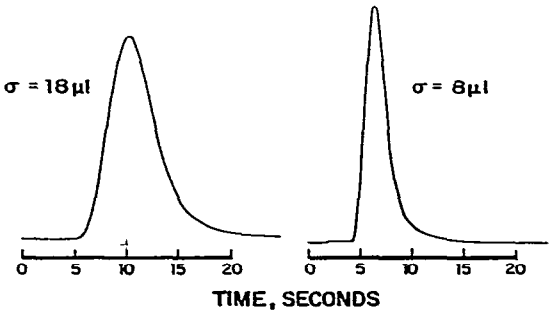

Fig. 10. Instrumental bandwidth measurement using different flowcells. Mobile phase: acetonitrile–water (65:35) at 0.5 ml/min. Sample: 6 μl uracil (20 μg/ml). UV detection at 254 nm; 8-μl flowcell on left and 2.4-μl flowcell on right.

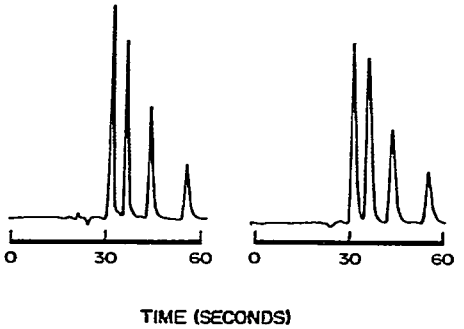

Fig. 11. Analysis of parabens using different flowcells. Column: 100 × 4.6 mm I.D., C_{18}-bonded phase, 3-μm particles. Mobile phase: acetonitrile–water (65:35) at 2.3 ml/min; inlet pressure: 3100 p.s.i.g. (22 MPa). Ambient temperature. UV detector at 254 nm. Peaks (in the sequence of their elution): methyl, ethyl, *n*-propyl, and *n*-butyl paraben. 8-μl flowcell on right and 2.4-μl flowcell on left. For data see Table V.

to 32 μl or a factor of about 2.2, or 4.8 in terms of variance. The influence of this on chromatographic performance is shown in Fig. 11 where a sample containing four parabens is separated on an instrumental system having the 2.4-μl flowcell, then on the same system but with the 2.4-μl flowcell replaced by the 8-μl flowcell. The improved efficiency resulting from use of the smaller cell is quite apparent and is more dramatic at lower k values. The efficiency data for these peaks are shown in Table V. The loss of efficiency resulting from use of the larger cell is from 40% on the last peak to 57% on the first peak.

TABLE V

INFLUENCE OF FLOWCELL VOLUME ON EFFICIENCY

Analytical conditions as in Fig. 11.

Solute	*k*	*Number of theoretical plates*		*Loss (%)*
		Cell volume (μl)		
		2.4	*8*	
Methyl paraben	0.7	5550	2380	57
Ethyl paraben	0.9	7220	2890	60
n-Propyl paraben	1.4	7640	3905	49
n-Butyl paraben	1.9	8310	4980	40

Detector response time

Several investigators have reported on the necessity for having a rapid detector response time in chromatography[19,27,29–33]. The requirements are even more demanding in high-speed LC since the parameters affecting the detector response time are all being altered such that a faster response is necessary. The time standard deviation of a peak σ_T can be determined as follows:

$$\sigma_T = \frac{(1 + k)\, V_0}{F\sqrt{n}} \tag{14}$$

where F is the volumetric flow-rate. For an unretained peak using the columns described above, where V_0 is approximately 750 μl and n is approximately 14,000 at a flow-rate of 3 ml/min, the time standard deviation of the unretained peak is about 127 msec. Therefore, a rapid response time is required so that the peak is not greatly distorted.

The advantage of using an active filter relative to a resistance–capacitance network has previously been discussed by Scott[33]. The active filter which has a sharper frequency cutoff (decibels/octave) is much more favorable for use in chromatography. The impulse response of the active filter we used is shown in Fig. 12. The total baseline response time is 135 msec. This corresponds to a time standard deviation of about 30 msec.

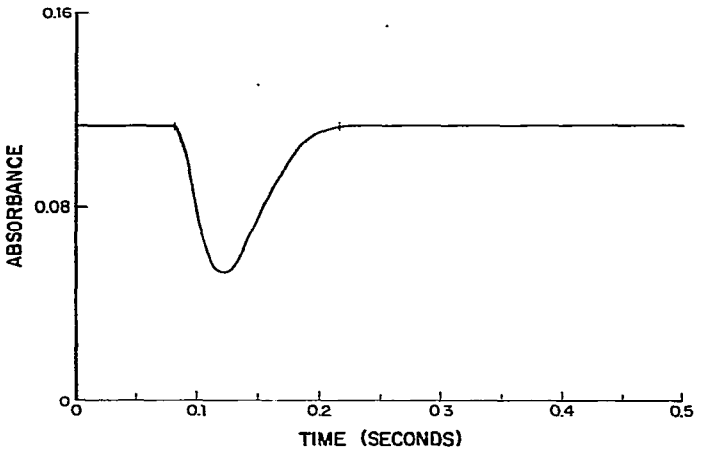

Fig. 12. Measurement of the instrumental response time. Absorbance is plotted as a function of time to measure the detector response to an instantaneous light pulse. The time required to return to the original light level is taken as the instrumental response time.

An added advantage to the use of an active filter as described above with its resulting gaussian-like profile is that it can be treated essentially as an independent gaussian operator on the system and its effect on the overall variance of the system determined easily as:

$$\sigma^2_{\text{DETECTOR}} = \sigma^2_{\text{FLOWCELL}} + (F\,\sigma_T)^2 \tag{15}$$

The active filter system in the detector has three selectable response times. These are 30, 300 and 3000 msec time standard deviation respectively. At flow-rates up to 10 ml/min (F = 167 μl/sec) the contribution to overall IBW by the fast filter is insignificant. However, at the medium response setting which is typical of conventional UV detector systems, we have observed losses of up to 65% in efficiency due to response time alone. These data are shown in Figs. 13 and 14. At a flow-rate of 6.6

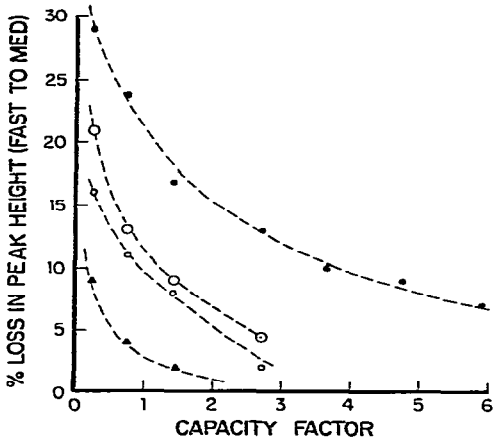

Fig. 13. Influence of the detector response time on the peak height. The percentage decrease in peak height using a 1.35-sec detector response time relative to a 0.135-sec response time is plotted against the capacity factor for various flow-rates. Column: 125 × 4.6 mm I.D., C_{18}-bonded phase packing, 5-μm particles. Mobile phase: acetonitrile–water (65:35); ambient temperature. Sample as in Table I. ▲, 3.3 ml/min (u = 5.7 mm/sec); ○, 4.4 ml/min (7.6 mm/sec); ⊙, 5.5 ml/min (9.6 mm/sec); ●, 6.6 ml/min (11.5 mm/sec).

ml/min (F = 110 μl/sec) a loss in peak height (Fig. 13) of approximately 30% resulted for the fastest eluting compound (k = 0.25). The loss in efficiency is even greater with losses of approximately 25% and 60% resulting at k values of 2.9 and 0.25, respectively (Fig. 14).

Recorders and data handling devices

The time constant requirements of high-speed LC on recording devices is quite similar to that of the detector. Since recorders with response times of 0.3–0.5 sec are readily available, band-broadening by the recorder only occurs if a faster responding

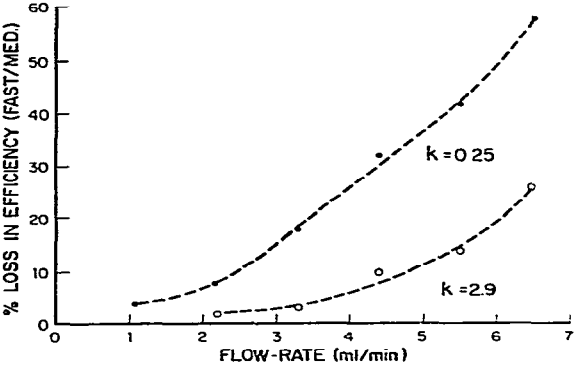

Fig. 14. Influence of detector response time on peak efficiency. The percentage decrease in peak efficiency (theoretical plate number) using a 1.35-sec detector response time relative to a 0.135-sec detector response time is plotted against the flow-rate for solutes with the respective capacity factors of k = 0.25 and 2.9. Column and conditions as in Fig. 13. Sample as in Table I.

detector is used. Band-broadening and loss of peak height is only apparent in extremely fast chromatographic traces from a LC-85 detector set at fast response. This effect is most apparent in normal-phase chromatography using low-viscoscity mobile phases where very high flow-rates are used. Comparing simultaneous traces from a Bascom Turner recorder at 100 data points/sec (which corresponds to a response time on the order of 10 msec) with that from a recorder (response time of 0.5 sec) for a very fast eluting peak with a half width of about 0.4 sec, we have observed an efficiency loss of up to 30% due to the recorder alone. This occurred at a mobile phase linear velocity of 20 mm/sec.

Perhaps of greater concern are the reproducibility of peak areas and retention times of data handling devices. This aspect is currently under investigation[34].

Gradient elution

High-speed columns with low void volumes are ideally suited for fast gradient analysis. This presents special problems since instruments with low gradient delay volumes are generally not available. We have previously demonstrated that a 3-min gradient can be achieved with excellent reproducibility with a specially designed solvent mixer[34]. Since high-speed columns can be completely equilibrated in 1–2 min, gradient cycle times can be less than 5 min. This permits rapid sample turnaround time in the gradient mode.

CONCLUSION

In conclusion we have described a LC system designed to utilize much of the potentials of small-dimensioned, small-particle columns. With this system performance levels of 300–450 plates/sec are obtainable thus permitting many useful analysis to be performed in 1–2 min with over 10,000 plates. Analysis of the instrumental bandwidth contribution of injector, connecting tubing, detector cell and electronic response shows that further improvements in reducing the instrumental bandwidths are required to realize the full potential of these small-particle columns.

LIST OF SYMBOLS

d_p	particle diameter
D_M	solute diffusivity in the mobile phase
F	mobile phase volumetric flow-rate
h	height equivalent to a theoretical plate, HETP
IBW	instrumental bandwidth
k	capacity factor
K	constant characteristic of the method of injection
L	column length
n	number of theoretical plates
n'	true number of theoretical plates of the column
N	number of effective plates
N'	true number of effective plates of the column
ΔP	pressure drop
r	tube radius

t_0 retention time of unretained peak
t_R retention time (from start)
u linear mobile phase velocity
V_{inj} injected sample volume
V_0 void volume of column
w_0 bandwidth at half height of the unretained peak
w_1 instrumental bandwidth at half height
w_{95} instrumental bandwidth
v $= n/t_R$
v' $= n'/t_R$
Y $= N/t_R$
Y' $= N'/t_R$
σ peak variance

REFERENCES*

1 J. L. DiCesare, M. W. Dong and L. S. Ettre, *Chromatographia*, 14 (1981) 257.
2 R. P. W. Scott and P. Kucera, *J. Chromatogr.*, 169 (1979) 51.
3 R. P. W. Scott, P. Kucera and M. Munroe, *J. Chromatogr.*, 186 (1979) 475.
4 C. E. Reese and R. P. W. Scott, *J. Chromatogr. Sci.*, 18 (1980) 479.
5 T. Tsuda and M. Novotny, *Anal. Chem.*, 50 (1978) 271.
6 M. Novotny, *J. Chromatogr. Sci.*, 18 (1980) 473.
7 D. Ishii, K. Asai, K. Hibi, T. Jonokuchi and M. Nagaya, *J. Chromatogr.*, 144 (1977) 157.
8 D. Ishii, T. Tsuda and T. Takeuchi, *J. Chromatogr. Sci.*, 18 (1980) 462.
9 J. H. Knox, *J. Chromatogr. Sci.*, 18 (1980) 453.
10 R. Tijssen, *Separ. Sci. Technol.*, 13 (1978) 681.
11 J. G. Atwood, G. J. Schmidt and W. Slavin, *J. Chromatogr.*, 171 (1979) 109.
12 D. H. Desty, A. Golup and W. T. Swanton, in N. Brenner, J. E. Callen and M. D. Weiss (Editors), *Gas Chromatography (1961 Lansing Symposium)*, Academic Press, New York, 1962, pp. 105–135.
13 I. Halász, R. Endele and J. Asshauer, *J. Chromatogr.*, 112 (1975) 37.
14 J. J. Kirkland, W. W. Yau, H. J. Stoklosa and C. H. Dilks, Jr., *J. Chromatogr. Sci.*, 15 (1977) 303.
15 E. Grushka, *Anal. Chem.*, 44 (1972) 1733.
16 G. I. Taylor, *Proc. Roy. Soc., Ser. A*, 219 (1953) 186.
17 J. G. Atwood and M. J. E. Golay, in preparation.
18 M. W. Dong, J. L. DiCesare and J. G. Atwood, unpublished results.
19 J. C. Sternberg, *Advan. Chromatogr.*, 2 (1966) 205.
20 J. F. K. Huber, J. A. R. J. Hulsman and C. A. M. Meijers, *J. Chromatogr.*, 62 (1971) 79.
21 B. Coq, G. Cretier, J. L. Rocca and M. Porthault, *J. Chromatogr. Sci.*, 19 (1981) 1.
22 B. L. Karger, M. Martin and G. Guiochon, *Anal. Chem.*, 46 (1974) 1640.
23 R. S. Deelder, M. G. F. Kroll, A. J. B. Beeren and J. H. M. van den Berg, *J. Chromatogr.*, 149 (1978) 669.
24 B. Coq, G. Cretier, C. Gonnet and J. L. Rocca, *Chromatographia*, 12 (1979) 139.
25 R. P. W. Scott and P. Kucera, *J. Chromatogr.*, 119 (1976) 467.
26 R. McNeil, *Anal. Chem.*, in press.
27 M. Martin, C. Eon and G. Guiochon, *J. Chromatogr.*, 108 (1975) 229.
28 R. P. W. Scott and P. Kucera, *J. Chromatogr. Sci.*, 9 (1971) 641.
29 J. W. Higgins, *J. Chromatogr.*, 148 (1978) 335.
30 G. K. C. Low and P. R. Haddad, *J. Chromatogr.*, 198 (1980) 235.

---

* *Editor's Note:* The same problem was solved in a different fashion by T. Takeuchi and D. Ishii (*J. Chromatogr.*, 213 (1981) 25). Their paper was submitted almost simultaneously to this manuscript. *Editor J. Chromatogr.*

31 L. J. Schmauch, *Anal. Chem.*, 31 (1959) 225.
32 I. G. McWilliam and H. C. Bolton, *Anal. Chem.*, 41 (1969) 1755.
33 R. P. W. Scott, *Liquid Chromatography Detectors*, Elsevier, Amsterdam, 1977, p. 46.
34 J. L. DiCesare and M. W. Dong, in preparation.